DOI:10.1021/jf903833a

JOURNAL OF AGRICULTURAL AND FOOD CHEMISTRY
ARTICLE

Terpenoids Induce Cell Cycle Arrest and Apoptosis from the Stems of *Celastrus kusanoi* Associated with Reactive Oxygen Species

Hui-Ling Chen,[†,⊥] Kai-Wei Lin,[†,⊥] A-Mei Huang,[‡,⊥] Huang-Yao Tu,[†] Bai-Luh Wei,[§] Tzyh-Chyuan Hour,[‡] Ming-Hong Yen,*[,†] Yeong-Shiou Pu,[∥] and Chun-Nan Lin*[,†,§]

[†]Faculty of Pharmacy, College of Pharmacy, Kaohsiung Medical University, Kaohsiung 807, Taiwan, [‡]Institute of Biochemistry, College of Medicine, Kaohsiung Medical University, Kaohsiung 807, Taiwan, [§]Department of Life Science, National Taitung University, Taitung 950, Taiwan, and [∥]Department of Urology, College of Medicine, National Taiwan University, Taipei 100, Taiwan. [⊥]These authors contributed equally to this work.

Bioguided fractionation of the $CHCl_3$ extracts obtained from *Celastrus kusanoi* stems led to isolation of two new terpenoids, 3β-hydroxy-11,14-oxo-abieta-8,12-diene (**1**) and 3β-*trans*-(3,4-dihydroxycinnamoyloxy)-11α-methoxy-12-ursene (**2**), and four known compounds characterized by spectroscopic methods. Compounds **1** and **2** and known triterpenoid erythrodiol (**3**) exhibited cytotoxic activity against bladder cancer cells (NTUB1) with IC_{50} values of 58.2 ± 2.3, 160.1 ± 60.9, and 18.3 ± 0.5 μM, respectively. Exposure of NTUB1 to **3** (5 and 10 μM) for 24 h significantly increased the level of production of reactive oxygen species (ROS). Flow cytometric analysis showed that treatment of NTUB1 with **3** led to the cell cycle arrest at G0/G1 accompanied by an increase in the extent of apoptotic cell death after 24 h. These data suggest that the presentation of G1 phase arrest and apoptosis in **3**-treated NTUB1 for 24 h was mediated through an increased amount of ROS in cells exposed to **3**.

KEYWORDS: ***Celastrus kusanoi*; terpenoids; cytotoxicity**

INTRODUCTION

The Celastraceae plants are rich in various sesquiterpene polyol esters, alkaloids, and terpenoids, some of which have exhibited an insect antifeedant effect, antitumor activity, multidrug resistance reversing activity, and anti-inflammatory activity (*1*). *Celastrus kusanoi* Hayata, Celastraceae, is distributed in China and Taiwan. The $CHCl_3$ extract of stems of *C. kusanoi* exhibited significant cytotoxic activity against several cancer cell lines. Bioactivity-guided fractionation has led to isolation of two new terpenoids, 3β-hydroxy-11,14-oxo-abieta-8,12-diene (**1**) and 3β-*trans*-(3,4-dihydroxycinnamoyloxy)-11α-methoxy-12-ursene (**2**), and four known compounds, including 28-hydroxy-β-amyrone (*2*, *3*), erythrodiol (**3**) (*4*), coniferaldehyde (*5*), and β-sitosteryl-3β-glucopyranoside-6′-*O*-palmitate (*6*), from the $CHCl_3$ extract of stems of *C. kusanoi*. In this work, structure elucidation of **1** and **2** and the cytotoxic activities of **1**−**3** (**Figure 1**) are reported.

MATERIALS AND METHODS

General Procedures. Optical rotations were recorded with a JASCO-370 polarimeter using appropriate solvent. UV spectra were recorded in MeOH on a JASCO UV−vis spectrophotometer. IR spectra were recorded on a Hitachi 260-30 spectrometer. ^1H (400 MHz) and ^{13}C NMR (100 MHz) spectroscopy and $^1H-^1H$ COSY, NOESY, HMQC, and HMBC experiments were conducted on a Varian Unity-400 NMR spectrometer. MS data were obtained on a JMS-HX-100 mass spectrometer.

Chemicals. Dimethyl sulfoxide (DMSO) was obtained from Merck. Cisplatin was obtained from Pharmacia & Upjohn (Milan, Italy). All culture reagents were obtained from Gibco BRL.

Plant Materials. The stems of *C. kusanoi* were collected at Ping Tung Hsieng, Taiwan, in August 2006. A voucher specimen (2006-E-1) has been deposited at the Department of Medicinal Chemistry, School of Pharmacy, Kaohsiung Medical University.

Extraction and Isolation. Dried stems of *C. kusanoi* (5 kg) were extracted three times (each with 20 L of $CHCl_3$) at room temperature for 6 months. The extracts were concentrated under reduced pressure to give a residue (40 g) that was subjected to column chromatography on silica gel and eluted with a C_6H_{12}/acetone gradient to afford 47 fractions that were combined into fractions **I**−**VIII**. Fraction **II**, eluted with a C_6H_{12}/acetone mixture (80:20), was purified on silica gel using a C_6H_{12}/acetone mixture (85:15) and further subjected to a series of normal phase MPLC separations to yield **1** (10 mg), β-28-hydroxy-β-amyrone (50 mg), and **3** (30 mg). Fraciton **III**, eluted with a C_6H_{12}/acetone mixture (67:33), was further purified by reverse phase MPLC using a MeOH/H_2O mixture (80:20) to afford **2** (7 mg). Finally, fraction **IV** (C_6H_{12}/acetone, 50:50) and fraction **V** (C_6H_{12}/acetone, 35:65) were subjected to repeated column chromatography and further purified on Sephadex LH-20 eluting with CH_3OH to give coniferaldehyde (15 mg) and β-sitosteryl-3-β-glucopyranoside-6′-*O*-palmitate

*To whom correspondence should be addressed. M.-H.Y.: e-mail, yen@kmu.edu.tw. C.-N.L.: telephone, +886 7 3121101; fax, +886 7 5562365; e-mail, lincna@cc.kmu.edu.tw.

 Published on Web 02/24/2010

(10 mg), respectively. The known compounds were identified using spectroscopic methods and gave values consistent with data reported in the literature (*2*−*6*).

3β-Hydroxy-11,14-oxo-abieta-8,12-diene (***1***)*:* yellow powder; $[\alpha]_D^{25}$ 55 (*c* 0.1, $CHCl_3$); UV(MeOH) λ_{max} (nm) (log ε) 269 (4.31); IR (KBr) ν_{max} 3228, 1649, 1599 cm^{-1}; ^1H and ^{13}C NMR data in **Table 1**; EIMS (70 eV) *m*/*z* 316 ($[M]^+$, 16), 298 (12), 283 (50), 241 (28), 91 (100); HREIMS *m*/*z* 316.2038 (calcd for $C_{20}H_{28}O_3$, 316.2036).

3β-trans-(3,4-Dihydroxycinnamoyloxy)-11α-methoxy-12-ursene (***2***)*:* white powder; $[\alpha]_D^{25}$ −52 (*c* 0.05, $CHCl_3$); UV (MeOH) λ_{max} (nm) (log ε) 226 (3.80), 302 (4.10), 330 (3.70); IR (KBr) ν_{max} 3366, 1695, 1597, 1519 cm^{-1}; ^1H and ^{13}C NMR data in **Table 1**; ESIMS *m*/*z* 641 $[M + Na]^+$, 517, 473, 457, 429; HRESIMS *m*/*z* 641.4186 $[M + Na]^+$ (calcd for $C_{40}H_{58}O_5Na$, 641.4182).

Cell Culture and MTT Assay for Cell Viability. NTUB1 human eurthelial carcinoma cells were maintained in RPMI 1640 medium supplemented with 10% fetal bovine serum (FBS), 100 units/mL penicillin G, 100 μg/mL streptomycin, and 2 mM L-glutamine. The cells were cultured at 37 °C in a humidified atmosphere containing 5% CO_2.

For evaluation of the cytotoxic effect of **1**−**3** and positive control cisplatin, a modified 3-(4,5-dimethylthiazol-2-yl)-2,5-diphenyltetrazolium bromide (MTT, Sigma Chemical Co.) assay was performed (*7*). Briefly, the cells were plated at a density of 1800 cells/well in 96-well plates and incubated at 37 °C overnight before being exposed to the drug. Cells were then cultured in the presence of graded concentrations of **1**−**3** and 10 μM cisplatin (Pharmacia & Upjohn) at 37 °C for 48 h. At the end of the culture period, 50 μL of MTT (2 mg/mL in PB) was added to each well and allowed to react for 3 h. Following centrifugation of plates at 1000*g* for 10 min, media were removed and 150 μL of DMSO was added to each well. The proportions of surviving cells were determined by absorbance spectrometry at 540 nm using an MRX (DYNEXCO) microplate reader. The cell viability was expressed as a percentage of the viable cells of the control culture condition. The IC_{50} values of each group were calculated by median effect analysis and presented as means ± the standard deviation (SD).

Flow Cytometry Analysis. DNA content was determined following propidium iodide (PI) staining of cells as previously described (*8*). Briefly, 8×10^5 cells were plated and treated with 10 μM cisplatin and various

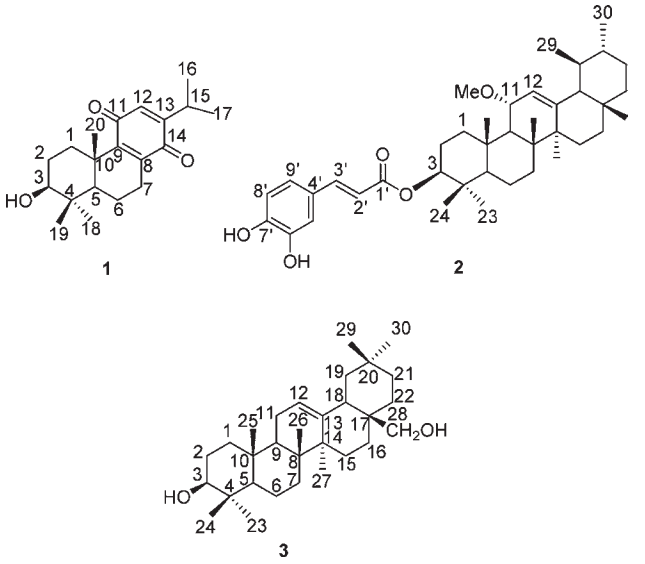

Figure 1. Structures of **1**−**3**.

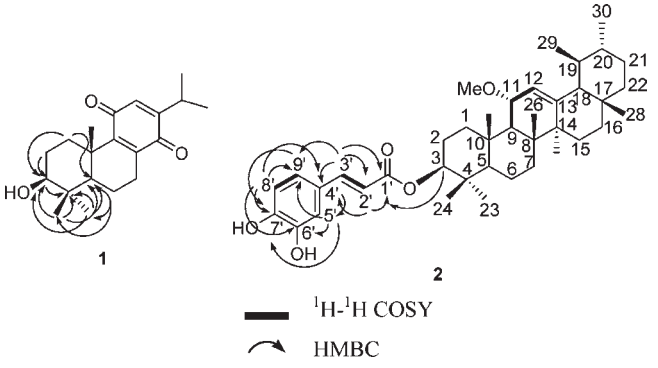

Figure 2. Key $^1H-^1H$ COSY and HMBC correlations of compounds **1** and **2**.

Table 1. ^1H and ^{13}C NMR Data for **1** and **2**

	1[a]		**2**[a]			**2**[a]	
	δ_H	δ_C	δ_H	δ_C		δ_H	δ_C
1	α 1.21 (m)	34.4	α 1.36 (m)	41.1	21	α 1.37 (m)	32.5
	β 2.80 (dt, 13.2, 3.5)		β 2.00 (m)			β 1.41 (m)	
2	1.73 (m)	27.7	α 1.62 (m)	25.4	22	α 1.36 (m)	42.8
			β 1.71 (m)			β 1.46 (m)	
3	3.25 (m)	78.3	4.58 (dd, 11.2, 5.0)	81.5	23	0.92 (s)	29.2
4		39.1		39.5	24	0.98 (s)	18.0
5	1.07 (m)	51.0	0.98 (m)	56.8	25	1.15 (s)	18.2
6	α 1.45 (m)	17.2	α 1.50 (m)	19.7	26	1.09 (s)	19.4
	β 1.88 (dd, 13.6, 7.6)		β 1.60 (m)		27	1.19 (s)	23.6
7	α 2.31 (ddd, 20.0, 11.2, 7.6)	26.2	α 1.32 (m)	34.7	28	0.84 (s)	29.8
			β 1.60 (m)		29	0.92 (d, 6.4)	18.5
8		142.8		44.4	30	0.93 (d, 6.4)	22.3
9		150.0	1.76 (m)	54.0	1′		167.9
10		38.2		39.5	2′	6.29 (d, 16.0)	116.8
11		187.9	3.82 (dd, 8.8, 2.8)	77.7	3′	7.54 (d, 16.0)	146.0
12	6.31 (s)	131.9	5.34 (d, 3.2)	126.0	4′		128.2
13		152.9		144.5	5′	7.16 (d, 2.0)	115.8
14		187.9		43.5	6′		147.1
15	2.79 (septet, 6.8)	26.3	1.78 (m)	28.2			
16	1.08 (d, 6.8)	21.3	0.92 (m)	29.3			
17	1.09 (d, 6.8)	21.3		34.9	7′		149.6
18	0.86 (s)	15.7	1.43 (bs)	59.9	8′	6.86 (d, 8.4)	117.0
19	1.04 (s)	28.2	1.41 (m)	41.0	9′	7.03 (dd, 8.4, 2.0)	123.1
20	1.27 (s)	20.1	2.01 (m)	40.8	OMe	3.26 (s)	55.3

[a] Measured in $CDCl_3$.

concentrations of **3** for 24 h, respectively. These cells were harvested by trypsinization, washed with 1× PBS, and fixed in ice-cold MeOH at −20 °C. After overnight incubation, the cells were washed with PBS and incubated with 50 μg/mL propidium iodide (Sigma Co.) and 50 μg/mL RNase A (Sigma Co.) in PBS at room temperature for 30 min. The fractions of cells in each phase of the cell cycle were analyzed using a FACScan flow cytometer and Cell Quest software (Becton Dickinson).

Quantitative Analysis of Intracellular Reactive Oxygen Species (ROS). Production of ROS was analyzed by flow cytometry as described previously (*9*). Briefly, cells were plated and treated under the indicated conditions. 2′,7′-Dichlorodihydrofluorescein diacetate (H_2DCFDA, 10 μM) (Molecular Probes, Eugene, OR) was added to the treated cells 30 min before they were harvested. The cells were collected by trypsinization and washed with PBS. The green fluorescence of intracellular DCF (2′,7′-dichlorofluorescein) was then analyzed immediately with a FACScan flow cytometer with a 525 nm band-pass filter (Becton Dickinson).

Statistical Analysis. Data were expressed as means ± SD. Statistical analyses were performed using the Bonferroni *t* test method after an ANOVA for multigroup comparison and the Student's *t* test method for a two-group comparison, where $p < 0.05$ was considered to be statistically significant.

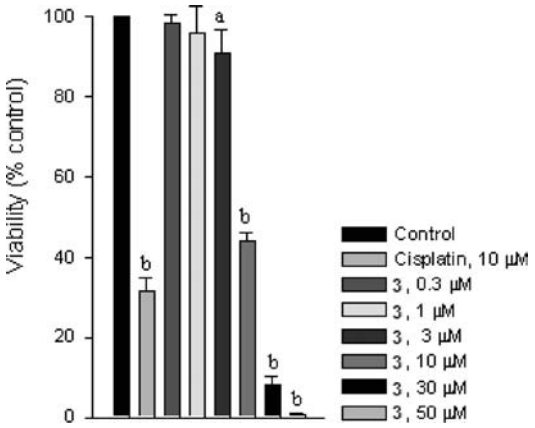

Figure 3. Compound **3** induced NTUB1 cell death. Cell viability was assessed by the MTT assay 48 h after treatment with different concentrations of **3**. $P < 0.05$ (a) and $P < 0.001$ (b) compared to the control value.

RESULTS AND DISCUSSION

Compound **1** was a yellow powder: $[\alpha]_D^{25}$ 55 (*c* 0.1, $CHCl_3$). Its HREIMS spectrum exhibited a $[M]^+$ peak at *m*/*z* 316.2038, corresponding to the molecular formula $C_{20}H_{28}O_3$ (calcd, 316.2036). The IR spectrum exhibited an absorption band for hydroxyl function (3328 cm^{-1}). The UV absorption at a λ_{max} of 269 nm (*10*) and the IR spectrum (1649, 1599 cm^{-1}) suggested the presence of a *p*-benzoquinone element (*11*). The ^{13}C NMR spectra (**Table 1**) were similar to that of tryptoquinone H (3,11,14-oxo-abieta-8,12 diene) (*12*) except for the carbon signals at C-2−C-4, C-18, and C-19. The ^1H NMR spectra (**Table 1**) are also very similar to that of tryptoquinone H except for the proton signals at H-2−H-5, Me-18, and Me-19. The HMBC correlations of H-1/C-3 and C-5, H-2/C-3, H-3/C-4, H-5/C-18 and C-19, Me-18/C-4 and C-5, Me-19/C-4, and C-5 and NOESY correlations between H_α-5/Me-18 and Me-18/H-3 (**Figure 2**) established **1** possessed a 3β-hydroxy-abietane-type diterpene. Hence, compound **1** was identified as 3β-hydroxy-11,14-oxo-abieta-8,12-diene (**1**).

Compound **2** was obtained as a white powder: $[\alpha]_D^{25}$ −52.0 (*c* 0.05, $CHCl_3$). Its HRESIMS spectrum exhibited an ion peak at

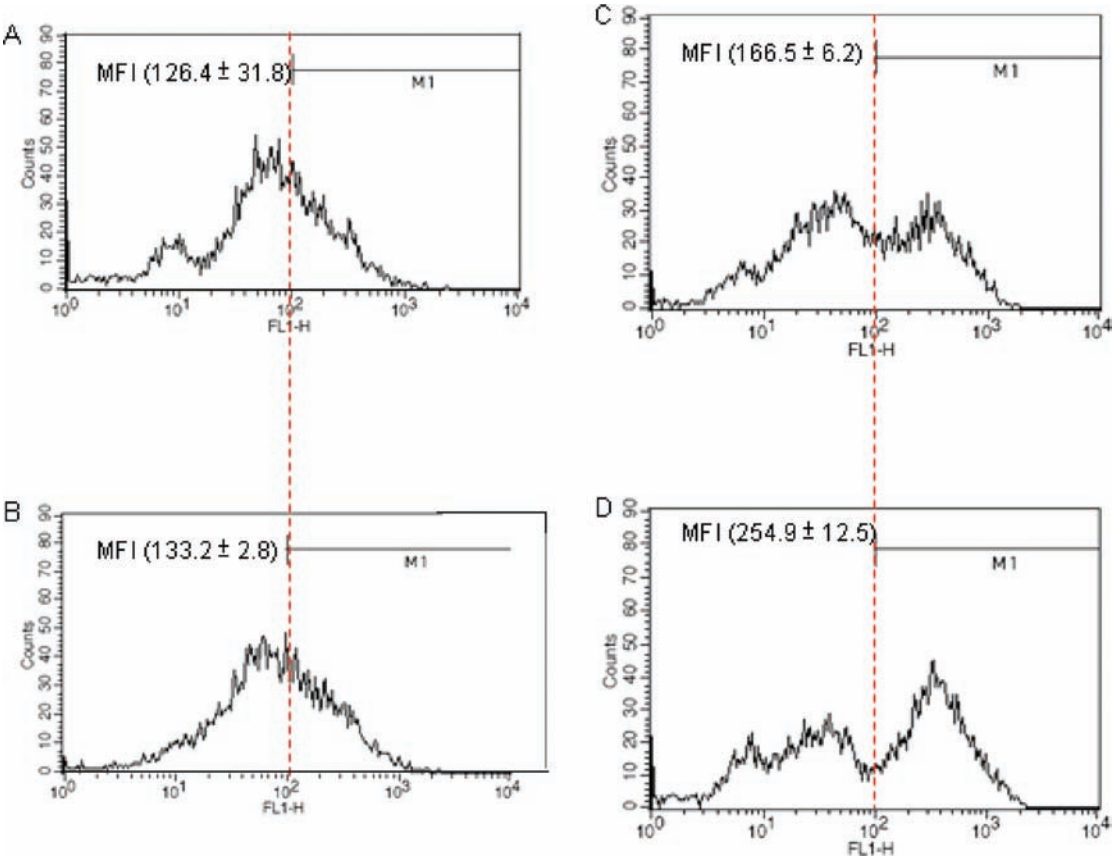

Figure 4. Effect of **3** on the production of ROS in NTUB1 cells: (**A**) control, (**B**) 10 μM cisplatin, (**C**) 5 μM **3**, and (**D**) 10 μM **3** for 24 h. The amount of ROS was assayed via H_2DCFDA staining. Each sampling measured the mean fluorescence intensity (MFI) of 3×10^5 cells cotreated via autofluorescence. The control cells were treated with medium. Three repeated experiments produced similar results.

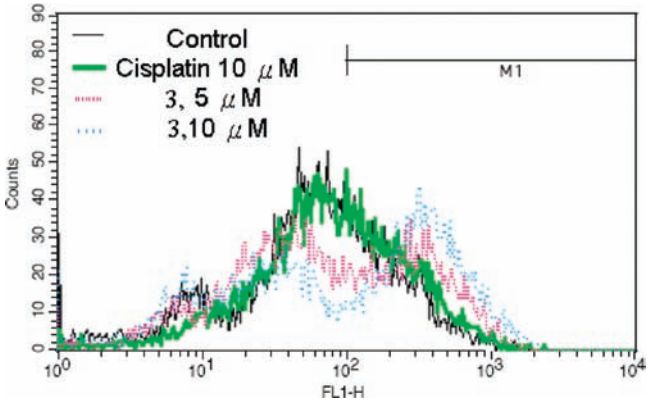

Figure 5. Effect of **3** and cisplatin in the production of ROS in NTUB1 cells. Cells were treated with 10 μM cisplatin and 5 and 10 μM **3** for 24 h, and the amount of ROS was assayed by H_2DCFDA staining. Three independent experiments produced similar results.

m/*z* 641.4186 consistent with the molecular formula $C_{40}H_{58}O_5Na$ $[M + Na]^+$ (calcd, 641.4182). The IR spectrum of **2** exhibited absorption bands that could be attributed to a hydroxyl group (3366 cm^{-1}), an α,β-unsaturated carbonyl ester (1695 cm^{-1}) (*13*), and an aromatic ring (1597, 1519 cm^{-1}), which together with the UV absorption at λ_{max} values of 226, 302, and 330 nm suggested the presence of a substituted cinnamoyl chromophore (*14*). The ^{13}C NMR spectra of **2** (**Table 1**) were similar to that of tryptohypol E (3β-hydroxy-11α-methoxy-12-ursene) (*12*) except for the presence of a downfield shift signal observed at C-3 and nine additional carbon signals (C-1′−C-9′). The ^1H NMR spectrum of **2** that exhibited a pattern of *trans* double bond proton signals at δ 6.29 (1H, d, J = 16.0 Hz, H-2′) and 7.54 (1H, d, J = 16.0 Hz, H-3′) and a 1,3,4-trisubstituted benzene proton with signals at δ 6.86 (1H, d, J = 8.4 Hz, H-8′), 7.03 (1H, dd, J = 8.4, 2.0 Hz, H-9′), and 7.16 (1H, d, J = 2.0 Hz, H-5′) revealed the presence of a phenylpropanoid ester moiety. The HMQC, $^1H-^1H$ COSY, and HMBC correlation shown in **Figure 2** established the structure of **2** as 3β-*trans*-(3,4-dihydroxycinnamoyloxy)-11α-methoxy-12-ursene (**2**).

Compounds **1**−**3** were evaluated for cytotoxic activity against the human NTUB1 cells. Cisplatin with an IC_{50} value of 3.27 ± 0.10 μM was used as a positive control in the cytotoxic assay. Compounds **1**−**3** exhibited cytotoxic activities with IC_{50} values of 58.2 ± 2.3, 160.1 ± 60.9, and 18.3 ± 0.5 μM, respectively. As shown in **Figure 3**, compound **3** at 10−50 μM caused a significantly increased level of NTUB1 cell death in a concentration-dependent manner.

ROS induce programmed cell death or necrosis, induce or suppress the expression of many genes, and activate cell signaling cascades (*15*). For further evaluation of the cytotoxic effect and mechanisms of induced cancer cell death in vitro, we first examined the effect of selective constituent **3** on the intracellular ROS level in NTUB1 cells. Expose of cells to 10 μM cisplatin and 5 and 10 μM **3** for 24 h caused a significant increase in the intracellular level of ROS as determined with the fluorescent dye, H_2DCFDA, which preferentially detected intracellular ROS (**Figures 4** and **5**).

ROS cause a wide range of adaptive cellular responses ranging from transient growth arrest to permanent growth arrest, apoptosis, or necrosis, depending on the amount of ROS. These responses allow organics to remove damage induced by ROS or allow cells to remove damage cells (*16*).

The effect of the positive control cisplatin and different concentrations of **3** on cell cycle progression was determined by using

Table 2. Cell Populations during the Cell Cycle of NTUB1 Cells[a] in the Presence of Cisplatin or **3**

	sub-G1	G0/G1	S	G2/M
control	3.29 ± 1.53	47.29 ± 4.18	23.24 ± 4.81	21.89 ± 2.34
10 μM cisplatin	2.30 ± 0.32	21.92 ± 1.07	56.02 ± 0.62	17.80 ± 0.61
5 μM **3**	3.21 ± 1.05	47.21 ± 5.60	25.05 ± 6.09	21.26 ± 1.98
10 μM **3**	3.19 ± 0.84	51.13 ± 6.45	23.54 ± 5.48	19.98 ± 2.75
20 μM **3**	6.48 ± 0.12	71.66 ± 0.30	7.35 ± 0.45	11.70 ± 0.33

[a] Flow cytometric analysis of the DNA histograms of propidium (PI)-stained NTUB1 cells in the presence of cisplatin or **3**. The cells were incubated with the indicated concentrations of cisplatin or **3**. After incubation, the cells were fixed and incubated with PI and RNase before the red fluorescence excited by blue light was read. The control contained cotreated cells. The cell populations of the cell cycle were analyzed with Lysis II.

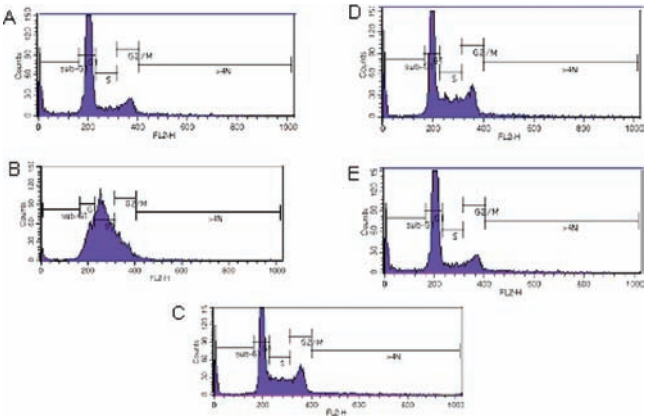

Figure 6. Flow cytometry analysis of cisplatin- and **3**-treated NTUB1 cells. NTUB1 cells (3×10^5 cells per 6 cm dish) were treated in the absence of cisplatin or compound: control (**A**), 10 μM cisplatin (**B**), 5 μM **3** (**C**), 10 μM **3** (**D**), or (**E**) 20 μM **3** for 24 h. At the indicated time, cells were stained with propidium iodide (PI), DNA contents were analyzed via flow cytometry, and the level of apoptosis was measured by the accumulation of sub-G1 DNA contents in cells. The control cells were treated with medium. Results are representative of three independent experiments.

fluorescence-activated cell sorting (FACS) analysis in propidium iodine-stained NTUB1 cells. As shown in **Table 2** and **Figures 6** and **7**, treatment with 5, 10, and 20 μM **3** for 24 h induced G1 phase arrest in a dose-dependent manner, accompanied by an increase in the level of apoptotic cell death. In the Chinese hamster ovary (CHO) cells, the cell cycle inhibition induced by H_2O_2 was accompanied by cell spreading and formation of focal adhesions during the early G1 phase (*17*). In the NTUB1 cells, the G1 phase arrest induced by **3** may also accompany cell spreading and formation of focal adhesions. This is valuable for the future study of the influence of cell spreading and formation of focal adhesions during G1 phase arrest induced by ROS.

Cellular ROS are known to be essential to cell survival, but the effect of ROS on cells is complex. Experimentally, a low concentration of H_2O_2 causes a moderate increase in the rate of proliferation of many tumor cell lines, whereas a higher level results in slowed growth, cell cycle arrest, and apoptosis or even necrosis (*18*). Treatment of cells with **3** for 24 h yielded G1 phase arrest and significantly increased the amount of ROS in cells. It indicated that the cell cycle arrest and apoptosis induced by **3** were correlated with ROS. Recently, compound **3** has been identified as a powerful inhibitor of 1321N1 astrocytoma cell growth and efficient apoptotic killing agent, and this suggested that the process is mediated by the activation of a ROS/JNK pathway (*19*). It indicated that the process of NTUB1 and 1321N1 cell death induced by **3** mediated through the increased production of ROS

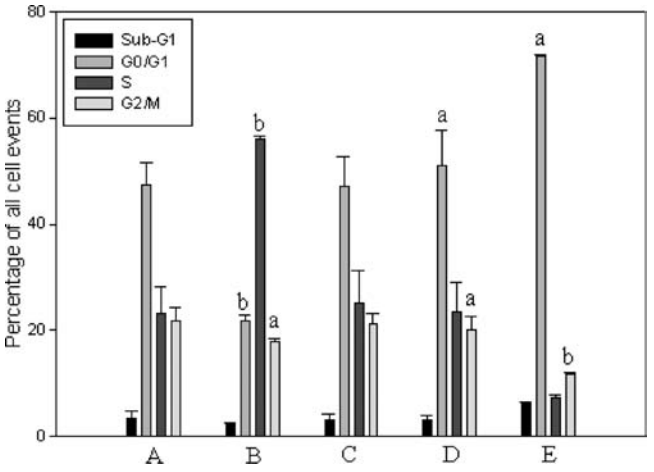

Figure 7. Cell cycle distribution of NTUB1 cells treated for 24 h with **3** at different concentrations. Cisplatin was used as a reference drug. Percentages of sub-G1 cells and cells in the G0/G1, S, and G2/M phases are shown. Data are from a representative experiment of three: (**A**) control, (**B**) 10 μM cisplatin, (**C**) 5 μM **3**, (**D**) 10 μM **3**, and (**E**) 20 μM **3**. $P < 0.05$ (a) and $P < 0.01$ (b) compared to the control values.

may be different. Further investigation should address the detailed mechanism of action inducing cell cycle arrest at the G1 phase and apoptosis.

In conclusion, two new cytotoxic terpenoids of *C. kusanoi* were isolated and characterized. A known triterpenoid **3** revealed a partial mechanism by which **3** mediated through generation of ROS in NTUB1 cells induction of G1 cell cycle arrest and apoptosis. Our study may not elucidate the detailed mechanism of **3**-induced inhibition of tumor cell growth but may encourage the development of novel, efficient, and less toxic anticancer agents targeting G1 phase arrest.

LITERATURE CITED

(1) Jin, H. Z.; Hwang, B. Y.; Kim, H. S.; Lee, J. H.; Kim, Y. H.; Lee, J. J. Antiinflammatory constituents of *Celastrus orbiculatus* inhibit the NF-κB activation and NO production. *J. Nat. Prod.* **2002**, *65*, 89–91.

(2) Monaco, P.; Caputo, R.; Palumbo, G.; Mangoni, L. Neutral triterpenes from the galls of *Pistacia terebinthus*. *Phytochemistry* **1973**, *12*, 939–942.

(3) Marner, F. J.; Freyer, A.; Lex, J. Triterpenoids from gum mastic, the resin of *Pistacia lentiscus*. *Phytochemistry* **1991**, *30*, 3709–3712.

(4) Nkengfack, A. E.; Formum, Z. T.; Ubillas, R.; Tempesta, M. S. A new prenylated isoflavone and triterpenoids from *Erythrina eriotriocha*. *J. Nat. Prod.* **1990**, *53*, 1552–1556.

(5) Sy, L.-K.; Brown, G. D. Coniferaldehyde derivatives from tissue culture of *Artemisia annua* and *Tanacetum parthenium*. *Phytochemistry* **1999**, *50*, 781−785.

(6) Pérezamador, M. C.; Jiménez, F. G. Corymbol, a new diterpenic acid. *Tetrahedron* **1966**, *22*, 1937–1942.

(7) Hour, T.-C.; Chen, J.; Huang, C.-Y.; Guan, J.-Y.; Lu, S.-H.; Hsieh, C.-Y.; Pu, Y.-S. Characterization of chemoresistance mechanisms in a series of cisplatin-resistant transitional carcinoma cell lines. *Anticancer Res.* **2000**, *20*, 3221–3225.

(8) Huang, A.-M.; Montagna, C.; Sharan, S.; Ni, Y.; Ried, T.; Sterneck, E. Loss of CCAAT/enhancer binding protein δ promotes chromosomal instability. *Oncogene* **2004**, *23*, 1549–1557.

(9) Pu, Y.-S.; Hour, T.-C.; Chen, J.; Huang, C.-Y.; Guan, J.-Y.; Lu, S.-H. Arsenic trioxide as a novel anticancer agent against human transitional carcinoma-characterizing its apoptotic pathway. *Anticancer Drugs* **2002**, *13*, 293–300.

(10) Scott, A. I. *Interpretation of the Ultraviolet Spectra of Natural Products*; Pergamon Press: Oxford, U.K., 1964; pp 101, 285.

(11) Mehrotra, R.; Vishwakarma, R. A.; Thakur, R. S. Abietane diterpenoids from *Coleus zeylanicus*. *Phytochemistry* **1989**, *28*, 3135–3137.

(12) Fujita, R.; Duan, H.; Takaishi, Y. Terpenoids from *Tripterigyum hypoglaucum*. *Phytochemistry* **2000**, *53*, 715–722.

(13) Bellamy, L. J. *The Infra-red Spectra of Complex Molecules*, 2nd ed.; Methuen & Co. Ltd.: London, 1958; p 149.

(14) Laphookhieo, S.; Karalai, C.; Ponglimanont, C.; Chantrapromma, K. Pentacyclic triterpenoid esters from the fruits of *Bruguiera cylindrical*. *J. Nat. Prod.* **2004**, *67*, 886–888.

(15) Hancock, J. T.; Desikan, R.; Neill, S. J. Role of reactive oxygen species in cell signaling pathway. *Biochem. Soc. Trans.* **2001**, *29* (Part 2), 345–350.

(16) Boonstra, J.; Post, J. A. Molecular events associated with reactive oxygen species and cell cycle progression in mammalian cells. *Gene* **2004**, *337*, 1–13.

(17) Munoz, C. M.; van Meeteren, L. A.; Post, J. A.; Verkleij, A. J.; Verrips, C. T.; Boonstra, J. Hydrogen peroxide inhibits cell cycle progression by inhibition of the spreading of mitotic CHO cells. *Free Radical Biol. Med.* **2002**, *33*, 1061–1072.

(18) Yi, J.; Yang, J.; He, R.; Gao, F.; Sang, H.; Tang, X.; Ye, R. D. Emodin enhanced arsenic trioxide-induced apoptosis via generation of reactive oxygen species and inhibition of survival signaling. *Cancer Res.* **2004**, *64*, 108–116.

(19) Martin, R.; Ibeas, E.; Carvalho-Tavares, J.; Hernández, M.; Ruiz-Gutierrez, V.; Nieto, M. L. Natural triterpenic diols promote apoptosis in astrocytoma cells through ROS-mediated mitochondrial depolarization and JNK activation. *PLoS One* **2009**, *4*, e5975.

Received for review November 7, 2009. Revised manuscript received February 7, 2010. Accepted February 9, 2010. This work was supported by a grant from the National Science Council of the Republic of China (NSC 94-2320-B-037-033).